Temperature dependences of optical properties, chemical composition, structure, and laser damage in Ta_2O_5 films*

Xu Cheng(许 程)[a)b)], Yang Shuai(杨 帅)[a)], Zhang Sheng-Hui(张生辉)[a)], Niu Ji-Nan(牛继南)[a)], Qiang Ying-Huai(强颖怀)[a)†], Liu Jiong-Tian(刘炯天)[b)], and Li Da-Wei(李大伟)[c)]

[a)] *School of Materials Science and Engineering, China University of Mining and Technology, Xuzhou* 221116, *China*

[b)] *School of Chemical Engineering & Technology, China University of Mining and Technology, Xuzhou* 221116, *China*

[c)] *Shanghai Institute of Optics and Fine Mechanics, Chinese Academy of Sciences, Shanghai* 201800, *China*

(Received 14 May 2012; revised manuscript received 29 May 2012)

Ta_2O_5 films are prepared by e-beam evaporation with varied deposition temperatures, annealing temperatures, and annealing times. The effects of temperature on the optical properties, chemical composition, structure, and laser-induced damage threshold (LIDT) are systematically investigated. The results show that the increase of deposition temperature decreases the film transmittance slightly, yet annealing below 923 K is beneficial for the transmittance. The XRD analysis reveals that the film is in the amorphous phase when annealed below 873 K and in the hexagonal phase when annealed at 1073 K. While an interesting near-crystalline phase is found when annealed at 923 K. The LIDT increases with the deposition temperature increasing, whereas it increases firstly and then decreases as the annealing temperature increases. In addition, the increase of the annealing time from 4 h to 12 h is favourable to improving the LIDT, which is mainly due to the improvement of the O/Ta ratio. The highest LIDT film is obtained when annealed at 923 K, owing to the lowest density of defect.

Keywords: Ta_2O_5 film, laser damage, deposition, annealing

PACS: 42.79.–e, 68.60.–p, 81.15.Dj **DOI:** 10.1088/1674-1056/21/11/114213

1. Introduction

The increasing demand for high-power laser systems in research, industrial, and defense applications calls for optical films witha high laser-induced damage threshold (LIDT). The mechanism of laser-induced damage has not been fully understood, as it is associated with many factors, such as deposition methods and conditions, substrates, laser characteristics, protective layers, and annealing.[1−6] The damage of films in the nanosecond laser pulse is always induced by defects; however, the detailed damage initiation is different and should be discussed for different cases.

As one of the most important optical film candidates, Ta_2O_5 has a large refractive index, a high adhesive force with substrates, and excellent thermal and chemical stability. The previous studies showed that the deposition temperature affected the properties of Ta_2O_5 films significantly. Jagadeesh Chandra *et al.* found that Ta_2O_5 films crystallized in the orthorhombic phase when the deposition temperature was above 673 K.[7] Kukli *et al.* prepared Ta_2O_5 films by atomic layer deposition, and detected the hexagonal phase when the deposition temperature was only 573 K.[8] In addition, Ta_2O_5 films are always substoichiometric in the conventional e-beam evaporation deposition process, which decreases the optical properties and the LIDT. Thereby, annealing is an important method for achieving better stoichiometry.[9]

In this paper, the main aim is to systematically investigate the effects of the deposition temperature, annealing temperature, and annealing time on the optical properties, chemical composition, structure, and LIDT of Ta_2O_5 films.

2. Experiment

Tetragonal Ta_2O_5 aggregates with a purity of 99.99% were used as the starting material. Before de-

*Project supported by the National Natural Science Foundation of China (Grant Nos. 61107080 and 50921002), the Natural Science Foundation of Jiangsu Province, China (Grant No. BK2011223), the Specialized Research Fund for the Doctoral Program of Higher Education of China (New Teachers) (Grant No. 20110095120018), the China Postdoctoral Science Foundation (Grant No. 20110491472), and the Fundamental Research Funds for the Central Universities, China (Grant No. 2012QNA03).

†Corresponding author. E-mail: yhqiang@cumt.edu.cn

© 2012 Chinese Physical Society and IOP Publishing Ltd

position, the chamber was pumped to a base pressure of 2×10^{-3} Pa, and oxygen was introduced to keep an oxygen partial pressure of 2×10^{-2} Pa. Ta_2O_5 films with the optical thickness of 6 QWOT (quarter wavelength optical thickness) at the wavelength of 550 nm were deposited by e-beam evaporation. Ten groups of Ta_2O_5 films were prepared, as listed in Table 1, and each group contained three samples deposited with the same condition. Groups 1–3 were deposited on BK7 substrates at room-temperature (RT), 473 K, and 573 K, respectively. Groups 4–7 were the films (573 K deposited, BK7 substrates) annealed at 573 K (4 h and 12 h) and 673 K (4 h and 12 h), respectively. Groups 8–10 were the films (573 K deposited, fused silica substrates) annealed for 8 h at 873 K, 923 K, and 1073 K, respectively. In groups 8–10, fused silica substrates were used, and the annealing time was reduced, as an annealing temperature higher than 673 K would weaken the properties of BK7. Transmittance spectra were measured using a Lambda 900 spectrophotometer; the measurement error was within 0.08%. The refractive indices were calculated by using the Essential Macleod (a thin film design software). The chemical compositions of the films were analyzed by X-ray photoelectron spectroscopy (XPS) using the focused monochromatic Al-$K\alpha$ ($h\upsilon$ = 1486.6 eV) radiation at a pass energy of 20 eV. The band gap of Ta_2O_5 was calculated using the first-principles pseudopotential method within the local density approximation. The structure was analyzed by using an X-ray diffractometer (XRD). The surface topography and the root mean square (RMS) roughness were obtained by a Nanocope III atomic force microscope (AFM). Damage testing was performed in the 1-on-1 regime according to ISO standard 11254-1 using a 1064 nm Q-switch pulsed laser at a pulse length of 12 ns.[10,11] The laser was focused to provide a far-field circular Gaussian beam with a diameter of 0.306 mm at $1/\mathrm{e}^2$ of the maximum intensity. The LIDT was defined as the incident pulse's energy density when the damage occurred with 0% damage possibility ($\mathrm{J/cm^2}$), and it could be obtained by the linear extrapolation of the damage possibility data to the zero damage possibility. Considering the test and the statistical errors, we estimated the total error to be about 12% in the LIDT measurement. The damage morphologies of the films were observed with a Leica-DMRXE microscope.

Table 1. Refractive index n_f (at 550 nm), packing density P, and O/Ta ratio of Ta_2O_5 films.

Group	Substrate	Deposition temperature/K	Annealing temperature/K	Annealing time/h	n_f	P	O/Ta ratio
1	BK7	RT	–	–	1.993	0.76	2.43
2	BK7	473	–	–	2.047	0.82	2.42
3	BK7	573	–	–	2.055	0.83	2.42
4	BK7	573	573	4	2.077	0.86	2.46
5	BK7	573	573	12	2.083	0.87	2.50
6	BK7	573	673	4	2.080	0.86	2.48
7	BK7	573	673	12	2.090	0.87	2.50
8	fused silica	573	873	8	2.092	0.88	2.50
9	fused silica	573	923	8	2.094	0.88	2.50
10	fused silica	573	1073	8	2.099	0.88	2.50

3. Results

Figure 1 shows the transmittance curves of the Ta_2O_5 films. Figure 1(a) illustrates that the transmittance decreases slightly with the increase of deposition temperature. The refractive indices are shown in Table 1, which increase with the temperature increasing. In fact, the deposition temperature is an important factor in the film growth process.[12,13] When the molecules are adsorbed on the substrate, the surface diffusion coefficient at equilibrium can be expressed by the Arrhenius equation

$$D(T) = D_0 \exp\left(-\frac{E}{k_\mathrm{B}T}\right), \tag{1}$$

where D_0 and E are the pre-exponential factors depending on the physical properties of the substrate deposit and the activation energy of the surface diffusion, respectively, k_B is the Boltzmann constant, and T is the deposition temperature in the deposition process.

From Eq. (1), it can be clearly seen that the higher the deposition temperature is, the larger the surface self-diffusion coefficient is. Therefore, it is easier for the molecules to diffuse at a higher deposition temperature, which results in the decrease of the film vacancies and the increase of the refractive index. Figures 1(b) and 1(c) show that when the annealing temperature increases in the range of 573–923 K, the transmittance increases. However, if the annealing temperature increases further to 1073 K, the transmittance would decrease obviously. The refractive index increases with the annealing temperature increasing, which could be attributed to the decrease of the structural vacancies by the thermal modification during annealing. The relation between the refractive index $n_{\rm f}$ and the packing density P can be illustrated as[14]

$$n_{\rm f} = Pn_{\rm s} + (1-P)n_{\rm v}, \tag{2}$$

where $n_{\rm s}$ and $n_{\rm v}$ are the refractive indices of the solid part of the film and the vacancies, respectively. Based on Eq. (2), the packing densities of Ta_2O_5 films are calculated as shown in Table 1. It shows that the packing density increases with the increasing deposition temperature, annealing temperature, and annealing time. The packing densities of Ta_2O_5 films deposited at room-temperature and 573 K are 0.76 and 0.83, respectively. The maximum packing density is 0.88 for the film annealed at 1073 K. Moreover, it indicates that there are many vacancies in the e-beam evaporated films, either before or after annealing.

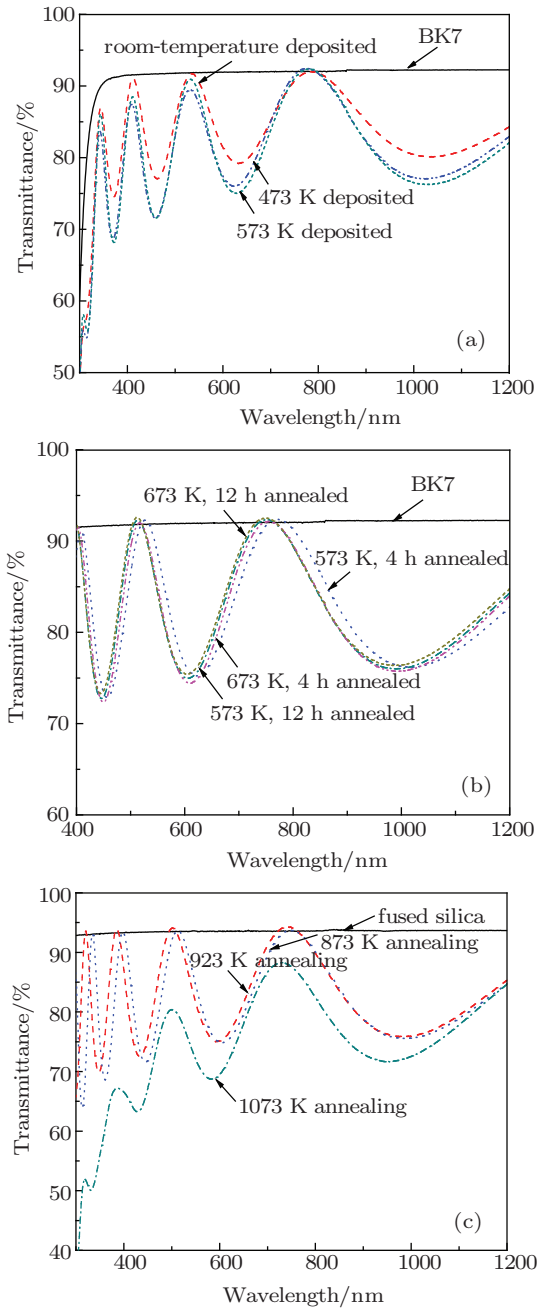


Fig. 1. (colour online) Transmittance of Ta_2O_5 films with (a) different deposition temperatures on BK7, (b) different annealing temperatures and annealing time on BK7, and (c) different annealing temperatures on fused silica.

A representative XPS survey scan in the range from 0 eV to 1400 eV of the Ta_2O_5 films is shown in Fig. 2(a). The peak at 284.8 eV corresponds to C 1s, owing to the contamination of the carbon on the surface, since they are exposed to the atmosphere. The survey spectrum shows the peak at the binding energy of 27 eV related to Ta 4f. The peaks observed at 230 eV and 242 eV correspond to Ta $4d_{5/2}$ and Ta $4d_{3/2}$, respectively. The peak located at 404 eV is attributed to Ta $4p_{3/2}$. The O 1s peak is observed at 531.5 eV. In addition, some impurities are found in the range of 975–1000 eV. Figure 2(b) shows the narrow scan XPS spectra in 23–32 eV for the as-deposited and the annealed Ta_2O_5 films. The spectra reveal $4f_{7/2}$ and $4f_{5/2}$ peaks at 26.4 eV and 28.2 eV, respectively, which shows that the composition of the films is Ta^{5+}. Figure 2(c) shows the two peaks fitted from the O 1s spectra, which illustrate the presence of different chemical environments. The lower binding energy peak at 530.6 eV is due to the Ta–O bonds, which indicates the presence of Ta_2O_5. The peak at 532.0 eV is usually attributed to the surface contamination.[15] The O/Ta ratio shown in Table 1 is estimated from the XPS peak areas together with their relative sensitivity factors. The relative sensitivity factors are 0.66 and 2.40 for O 1s and Ta 4f, respectively. On the whole, the O/Ta ratio decreases slightly with the deposition temperature increasing, which indicates the increase of the film absorption. The O/Ta ratio of the film annealed at 573 K for 12 h is 2.50, whereas it is

2.48 for the film annealed at 673 K for 4 h. It indicates that the O/Ta ratio of the Ta_2O_5 films depends not only on the annealing temperature, but also on the annealing time. In addition, all the films annealed above 673 K for 8 h are stoichiometric. Moreover, as the O/Ta ratio is less than 2.50, the substoichiometric defects in the Ta_2O_5 films are oxygen vacancies.

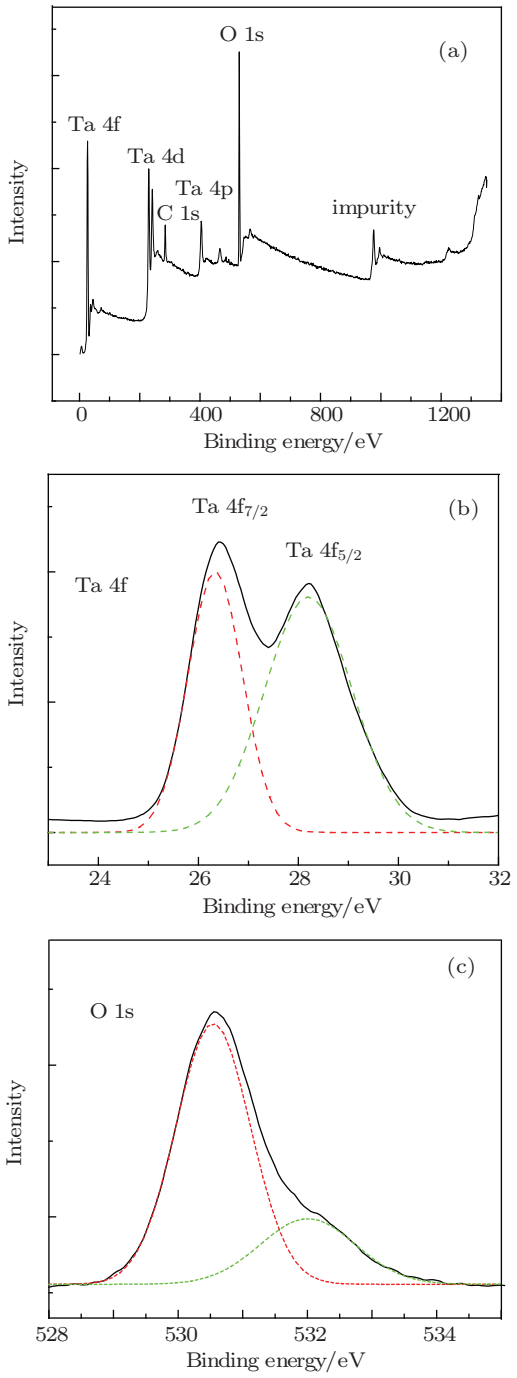


Fig. 2. (colour online) Typical XPS (a) survey scan and ((b), (c)) narrow scans of Ta_2O_5 films.

For the band gap calculation, the program CASTEP (Cambridge Serial Total Energy Package) is used,[16] which is based on the density functional theory (DFT) in describing the electron–electron interaction and a pseudopotential description of the electron–core interaction. For the exchange–correlation term, the local density approximation is used. As crystalline Ta_2O_5 is usually used to calculate the band gap, Ta_2O_5 of the C12/c1 space group is chosen in this paper. The lattice constants are $a = 12.7853$, $b = 4.8537$, $c = 5.5276$, $\alpha = \gamma = 90$, and $\beta = 104.264$. A 2×2×1 supercell is built, as shown in Fig. 3(a). The energy cutoff is set at 340 eV. The k-point grid is set to be 3×3×3. The results show that the band gap of Ta_2O_5 is 2.54 eV, which is consistent to the previous results.[4,17] However, it is much smaller than the experimental band gap of Ta_2O_5 (4.3 eV). This discrepancy is related to the DFT method, which often underestimates the band gap values.

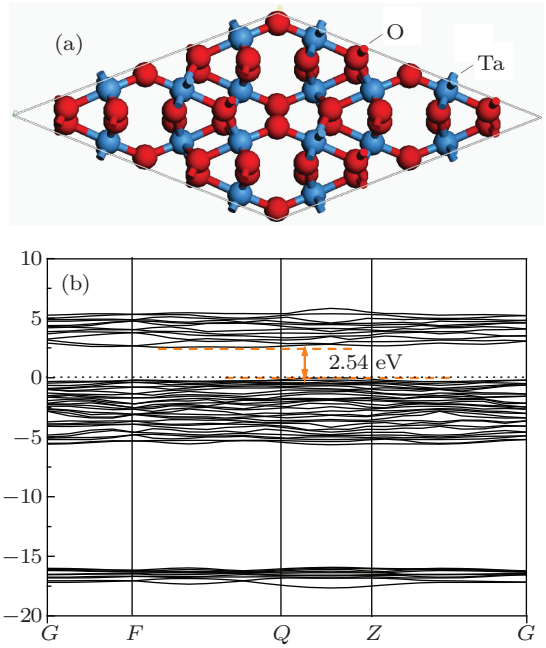


Fig. 3. (colour online) (a) The 2×2×1 supercell and (b) the microscopic band gap of Ta_2O_5.

To explore the effect of a substoichiometric chemical composition on the band gap, the partial occupancies of oxygen are used to simulate firstly. This approach treats all oxygen sites in each unit cell equivalently, and is a type of mean-field approach, which is called the virtual crystal approximation.[18] Therefore, the O/Ta ratios of 2.42, 2.43, 2.46, and 2.48 are in correspondence with the oxygen occupations of 0.968, 0.972, 0.984, and 0.992, respectively. The calculated band gap is shown in Fig. 4. The results indicate that the substoichiometric chemical composition plays a little effect on the band gap.

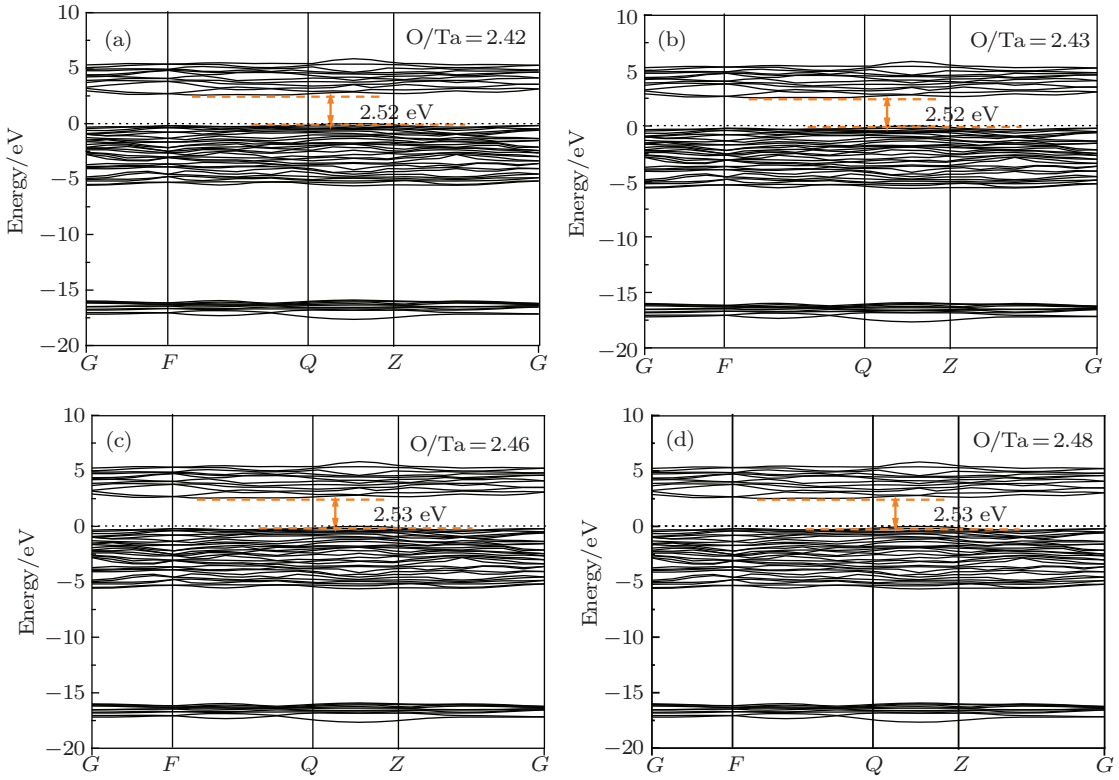


Fig. 4. (colour online) The band gaps of Ta_2O_5 with O/Ta ratios of (a) 2.42, (b) 2.43, (c) 2.46, and (d) 2.48.

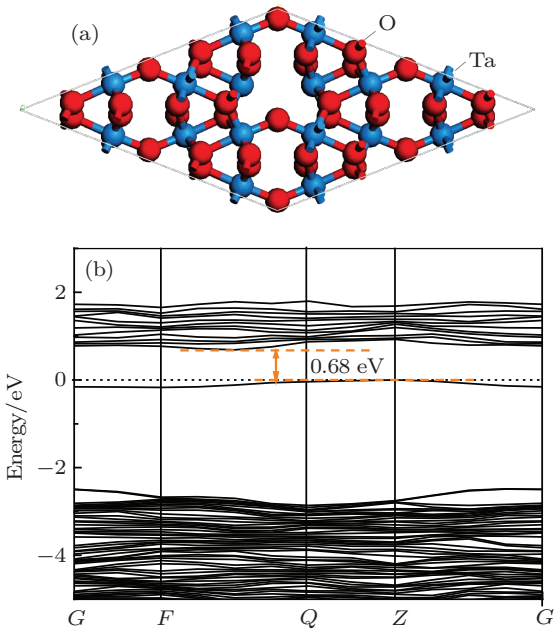


Fig. 5. (colour online) (a) The 2×2×1 supercell and (b) the band gap of Ta_2O_5 with oxygen vacancy.

It is worth noting that the above simulation has some limits, as the actual situation of the substoichiometry of Ta_2O_5 is the existence of oxygen vacancies, according to the XPS results. Thus, the oxygen atom at the center of the 2×2×1 Ta_2O_5 supercell is removed, as shown in Fig. 5 (a). Figure 5 (b) shows that the calculated band gap is 0.68 eV. It indicates that once the oxygen vacancy forms, the band gap decreases 73%.

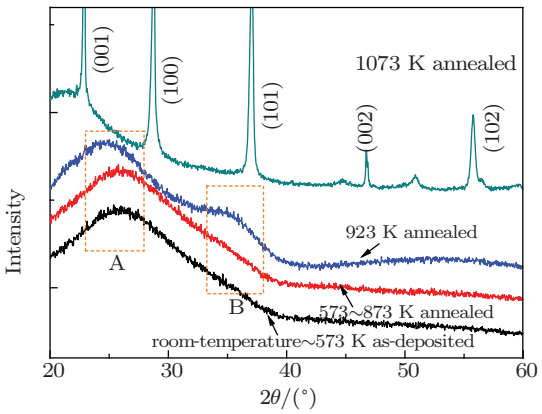


Fig. 6. (colour online) XRD analysis of Ta_2O_5 films.

Figure 6 illustrates that the films are amorphous when deposited below 573 K and annealed below 873 K. As the annealing temperature increases to 1073 K, the film crystallizes in the hexagonal phase. An interesting phenomenon is that areas *A* and *B* in

Fig. 6 show the position change and the intensity increase when annealed at 923 K. It indicates the crystalline trend of the film. Therefore, we can call it the near-crystalline phase, which means between the amorphous phase and the crystalline phase.

Figure 7 demonstrates the surface topographies of room-temperature deposited, 473 K deposited, 923 K annealed, and 1073 K annealed films. It displays that the surface topography depends on the depositing temperature, the annealing temperature, and the annealed time. The RMS roughness of Ta_2O_5 films is shown in Fig. 8. It reveals that the deposition temperature has little effect on the RMS. In addition, when annealed in the range of 573–923 K, the RMS roughness of the film changes slightly. However, when the annealing temperature increases to 1073 K, the RMS increases significantly, which could be attributed to the crystallization of the Ta_2O_5 films, as shown in Fig. 6. Meanwhile, as the crystal grows up rapidly in the phase transition process, some microcracks are easily found on the film's surface by the naked eye.

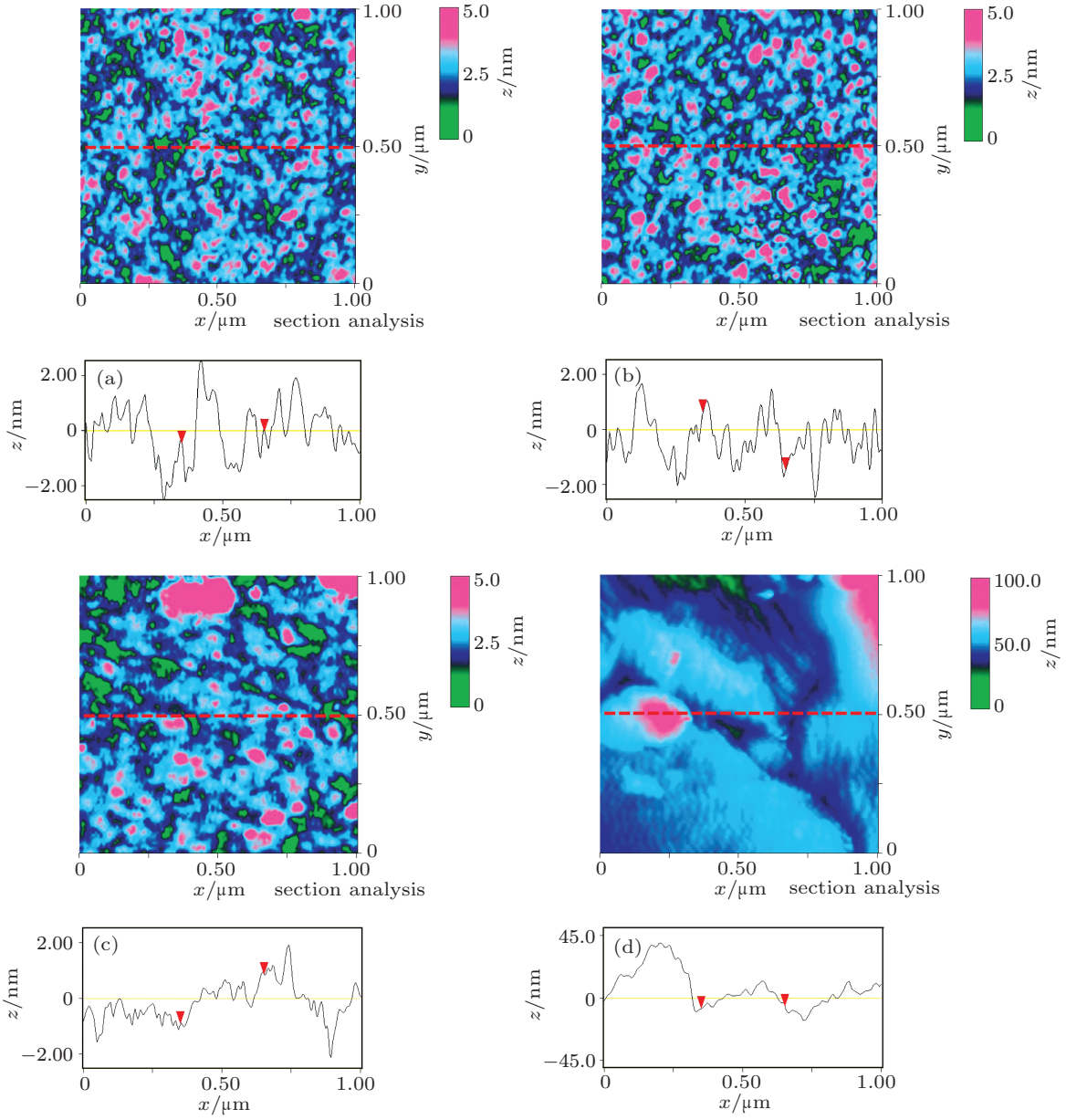


Fig. 7. (colour online) AFM images of groups (a) 1, (b) 2, (c) 9, and (d) 10.

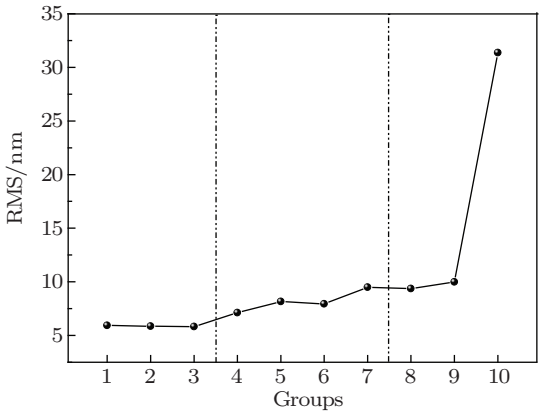


Fig. 8. RMS roughness of Ta_2O_5 films.

Figure 9 shows the LIDTs of the Ta_2O_5 films. It reveals that the LIDT increases with the increase of the deposition temperature, whereas it increases firstly and then decreases as the annealing temperature increases. In addition, all the LIDTs of the as-deposited films are smaller than those of the annealed films. Moreover, it can be seen that the film annealed at 673 K for 4 h (group 6) achieves a lower LIDT than the film annealed at 573 K for 12 h (group 5), which indicates that the LIDT is affected by the combination of annealing temperature and annealing time.

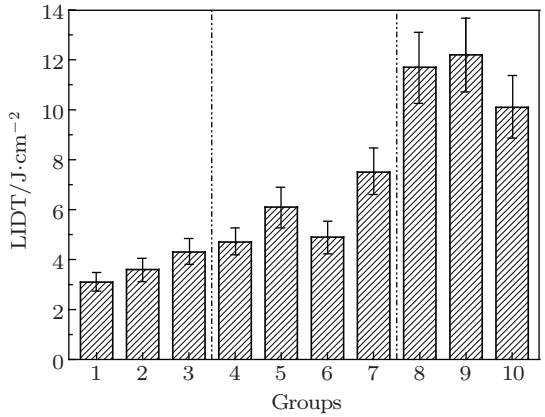


Fig. 9. The LIDTs of Ta_2O_5 films.

The typical bright-field microscopy image of damage morphology is shown in Fig. 10. It illustrates the absorption centers in the damaged area, which reveals that the damage initiates from the defects. It is consistent with the defect-induced mechanism, as the defect has a larger absorbance index than the film around, it is more liable to absorb the laser energy and results in damage.

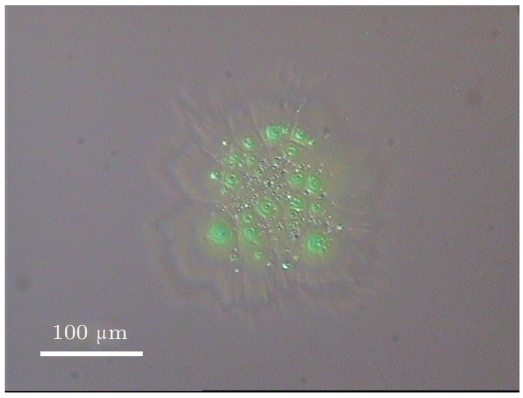


Fig. 10. (colour online) Typical damage morphology of Ta_2O_5 films.

4. Discussion

The experimental results evidently show that the temperature affects the optical properties, chemical composition, structure, and LIDT of the Ta_2O_5 films. In the following, the effects of temperature on the LIDT will be especially discussed. The laser damage in the nanosecond region always arises as a result of strong absorption points induced by the defects. The previous results showed that the defects can be divided into two kinds: one is the structural defects, such as big structural vacancies, nodular defects, grain boundaries, and microcracks, and the other is the substoichiometric defect.[19,20] In addition, the adhesive force, the intrinsic absorption, and the melting point also influence the LIDT.[21,22] The discussion about the different effects of the deposition temperature, annealing temperature, and annealing time on the LIDT is given in the following.

(i) With the increasing deposition temperature, the packing density increases, and the film vacancies decrease. Therefore, the density of the structural defect decreases, contributing to the LIDT improvement. Moreover, the increase of the packing density will also be favourable to enhancing the adhesive force between aggregations in the films, which is also beneficial for the LIDT.

(ii) The LIDT of the annealed films is higher than that of the as-deposited films, which can be explained as follows. The O/Ta ratio of the as-deposited Ta_2O_5 films is less than 2.50, indicating the films are substoichiometric. The activation energy of the substoichiometric defect is only 0.6 eV, so this defect is very easy to turn into the damage center under laser radiation.[23] Moreover, as shown in Figs. 3 and 5, the band gap of Ta_2O_5 is 2.54 eV, and it decreases 73%

to 0.68 eV when the oxygen vacancy forms. The serious decrease of the microscopic band gap may significantly increase the absorbance of the micro areas in films when irradiated by a laser, thus the damage probability increases. So the damage of the as-deposited films is mainly induced by this kind of defect, and the LIDT is low. In the annealing process, as the Gibbs free energy of the reaction of oxygen and nonoxidized Ta inside the film is negative, it is favourable for this reaction to occur based on thermodynamical arguments.[24] During annealing, the oxygen penetrates and reacts with the substoichiometic films, improving the film stoichiometry and decreasing the density of the substoichiometric defect. Moreover, the effects of annealing are similar to the increase of the deposition temperature, as it provides the thermal energy to drive the atoms to modify and diffuse, decreasing the density of the structural defect and enhancing the adhesive force. Therefore, annealing improves the LIDT significantly.

(iii) The LIDT increases firstly with the increase of the annealing temperature, and the film annealed at 923 K achieves the LIDT of 12.2 J/cm^2. Then it decreases to 10.1 J/cm^2 when the temperature increases to 1073 K. It reveals that the effects of the annealing temperature on the LIDT are more complicated than the deposition temperature effects. It is worth noting that both the O/Ta ratios of the films annealed at 923 K and 1073 K are 2.50, so there is no substoichiometric defect. The most obvious difference in the two films is that the former is in the near-crystalline phase and the later is in the crystalline phase. Therefore, the decrease of LIDT is due to the increased density of structural defects, such as the grain boundaries and the microcracks, during the phase transition process. In addition, the LIDT of the film annealed at 923 K is higher than that annealed at 873 K, which might mean that the former also has fewer defects than the later.

(iv) The effects of annealing on the film properties depend not only on the annealing temperature, but also on the annealing time. The results show that the 12 h annealed films have higher LIDTs than the 4 h annealed films. In this experiment, groups 5 and 7 have higher LIDTs than groups 4 and 6, increasing 29.8% and 53.1%, respectively. It is attributed to the disappearance of the substoichiometric defect, as the O/Ta ratio increases to 2.50. Meanwhile, the increase of the annealing time decreases the density of the structural defects, also contributing to the improvement of the LIDT. In addition, the film annealed at 573 K for 12 h (group 5) achieves a higher LIDT than the film annealed at 673 K for 4 h (group 6) mainly owning to the disappearance of the substoichiometric defect.

5. Conclusion

In summary, the effects of the deposition temperature, annealing temperature, and annealing time on the optical properties, chemical composition, structure, and LIDT of the Ta_2O_5 films have been investigated in this paper. The results show that the increase of the deposition temperature decreases the film transmittance slightly, yet annealing below 923 K is beneficial for the transmittance. The O/Ta ratio depends not only on the annealing temperature, but also on the annealing time. The LIDT increases with both the increasing deposition temperature and the increasing annealing time, whereas it increases firstly and then decreases with the increasing annealing temperature. Moreover, the LIDT is affected by the combination of the annealing temperature and annealing time. The highest LIDT film will be obtained when annealed at 923 K owing to the lowest density of defect.

References

[1] Liu Z, Chen S, Ma P, Wei Y, Zheng Y, Pan F, Liu H and Tang G 2012 *Opt. Express* **20** 854

[2] Xia Z, Zhao Y, Huang C, Xue Y and Guo P 2009 *Opt. Commun.* **282** 970

[3] Xu C, Xiao Q, Ma J, Jin Y, Shao J and Fan Z 2008 *Appl. Surf. Sci.* **254** 6554

[4] Yu H, Qi H, Cui Y, Shen Y, Shao J and Fan Z 2007 *Appl. Surf. Sci.* **253** 6113

[5] Han W, Wang F, Zhou L, Feng B, Jia H, Li K, Xiang Y and Zheng W 2012 *Chin. Phys.* B **21** 077901

[6] Jiang Y, Xiang X, Liu C, Luo C, Wang H, Yuan X, He S, Ren W, Lv H, Zheng W and Zu X 2012 *Chin. Phys.* B **21** 064219

[7] Jagadeesh Chandra S V, Uthanna S and Mohan Rao G 2008 *Appl. Sur. Sci.* **254** 1953

[8] Kukli K, Rital M, Matero R and Leskelä M 2000 *J. Cryst. Growth* **212** 459

[9] Wolfe C R, Kozlowski M R, Campbell J H, Rainer F, Morgan A J and Gonzales R P 1989 *Proc. SPIE* **509** 255

[10] Hu H, Fan Z and Luo F 2001 *Appl. Opt.* **40** 1950

[11] ISO 11254-1:2000: *Lasers and Laser-related Equipment-Determination of Laser-induced Damage Threshold of Optical Surfaces.* Part 1. 1-on-1 test

[12] Boulouz M, Boulouz A, Giani A and Boyer A 1998 *Thin Solid Films* **323** 85

[13] Yu H, Shen Y, Cui Y, Qi H, Shao J and Fan Z 2008 *Appl. Surf. Sci.* **254** 1783

[14] Macleod H A 1986 *J. Vac. Sci. Technol.* A **4** 418

[15] Atanassova E, Spassov D, Paskaleva A, Koprinarova J and Georgieva M 2002 *Microelectron. J.* **33** 907

[16] Payne M C, Teter M P, Allan D C, Arias T A and Joannopoulos J D 1992 *Rev. Mod. Phys.* **64** 1045

[17] Fleming R M, Lang D V, Jones C D W, Steigerwald M L, Murphy D W, Alers G B, Wong Y H, van Dover R B, Kwo J R and Sergent A M 2000 *J. Appl. Phys.* **88** 850

[18] Sainz-Diaz C I, Hernandez-Laguna A and Dove M T 2001 *Phys. Chem. Minerals* **28** 130

[19] Zhao Y, Gao W, Shao J and Fan Z 2004 *Appl. Surf. Sci.* **227** 275

[20] Xu C, Ma J, Jin Y, He H, Shao J and Fan Z 2008 *Chin. Phys. Lett.* **25** 1321

[21] Xu C, Qiang Y, Zhu Y, Shao J, Fan Z and Han J 2010 *Opt. Laser Technol.* **42** 497

[22] Yuan L, Zhao Y, Shang G, Wang C, He H, Shao J and Fan Z 2007 *J. Opt. Soc. Am.* B **24** 538

[23] Sawada H and Kawakami K 1999 *J. Appl. Phys.* **86** 956

[24] Shinriki H, Kisu T, Kimura S, Nishioka Y, Kawamoto Y and Mukai K 1990 *IEEE Trans. Electron Devices* **37** 1939